Inorg. Chem. **2002**, *41*, 2229–2237

Inorganic Chemistry
Article

Synthesis, Characterization, and Chiral Behavior of S-Bridged $Co^{III}Pt^{II}Co^{III}$ Trinuclear Complexes Composed of Bis(thiolato)-Type Octahedral Units *cis*(*S*)-$[Co(aet)_2(en)]^+$ and/or *trans*(*N*)-$[Co($D-pen-*N*,*O*,*S*$)_2]^-$ (aet = 2-Aminoethanethiolate, D-pen = D-Penicillaminate)

Hirokazu Honda,[†] Takashi Yoshimura,[‡] Masakazu Hirotsu,[‡] Tatsuya Kawamoto,[†] and Takumi Konno*,[†]

Departments of Chemistry, Graduate School of Science, Osaka University,
Toyanaka, Osaka 560-0043, Japan, and Faculty of Engineering, Gunma University,
Kiryu, Gunma 376-8515, Japan

Received July 2, 2001

A series of linear-type $Co^{III}Pt^{II}Co^{III}$ trinuclear complexes composed of C_2-*cis*(*S*)-$[Co(aet)_2(en)]^+$ (aet = 2-aminoethanethiolate) and/or Λ_D-*trans*(*N*)-$[Co($D-pen-*N*,*O*,*S*$)_2]^-$ (D-pen = D-penicillaminate) were newly prepared, and their chiral behavior, which is markedly different from that of the corresponding $Co^{III}Pd^{II}Co^{III}$ complexes, is reported. The 1:1 reaction of an S-bridged $Co^{III}Ni^{II}Co^{III}$ trinuclear complex, $[Ni\{Co(aet)_2(en)\}_2]Cl_4$, with $K_2[PtCl_4]$ in water gave an S-bridged $Co^{III}Pt^{II}Co^{III}$ trinuclear complex, $[Pt\{Co(aet)_2(en)\}_2]Cl_4$ ([**1**]Cl_4), while the corresponding 1:2 reaction produced an S-bridged $Co^{III}Pt^{II}$ dinuclear complex, $[PtCl_2\{Co(aet)_2(en)\}]Cl$ ([**2**]Cl). Complex $[\mathbf{1}]^{4+}$ formed both racemic ($\Delta\Delta/\Lambda\Lambda$) and meso ($\Delta\Lambda$) forms, which were separated and optically resolved by cation-exchange column chromatography. An optically active S-bridged $Co^{III}Pt^{II}Co^{III}$ trinuclear complex having the pseudo $\Lambda\Lambda$ configuration, $\Lambda_D\Lambda_D$-$[Pt\{Co($D-pen-*N*,*O*,*S*$)_2\}_2]^0$ ($\Lambda_D\Lambda_D$-[**3**]), was also prepared by reacting Λ_D-*trans*(*N*)-K$[Co($D-pen-*N*,*O*,*S*$)_2]$ with $K_2[PtCl_4]$ in a ratio of 2:1 in water. Treatment of the racemic Δ/Λ-[**2**]Cl with Λ_D-*trans*(*N*)-K$[Co($D-pen-*N*,*O*,*S*$)_2]$ in a ratio of 1:1 in water led to the formation of $\Lambda\Lambda_D$- and $\Delta\Lambda_D$-$[Pt\{Co(aet)_2(en)\}\{Co($D-pen-*N*,*O*,*S*$)_2\}]^{2+}$ ($\Lambda\Lambda_D$- and $\Delta\Lambda_D$-$[\mathbf{4}]^{2+}$) and $\Delta\Delta_D$-$[Pt\{Co(aet)_2(en)\}\{Co($D-pen-*N*,*S*$)_2(H_2O)_2\}]^{2+}$ ($\Delta\Delta_D$-$[\mathbf{4'}]^{2+}$), besides trace amounts of $\Lambda_D\Lambda_D$-[**3**] and $\Delta\Delta$- and $\Delta\Lambda$-$[\mathbf{1}]^{4+}$. These $Co^{III}Pt^{II}Co^{III}$ complexes were characterized on the basis of electronic absorption, CD, and NMR spectra, along with single-crystal X-ray analyses for $\Delta\Delta/\Lambda\Lambda$-[**1**]$Cl_4$, $\Delta\Lambda$-[**1**]Cl_4, and $\Delta\Lambda_D$-[**4**]Cl_2. Crystal data: $\Delta\Delta/\Lambda\Lambda$-[**1**]$Cl_4\cdot6H_2O$, monoclinic, space group *C*2/*c* with $a = 14.983(3)$ Å, $b = 19.857(4)$ Å, $c = 12.949(3)$ Å, $\beta = 113.51(2)°$, $V = 3532(1)$ Å^3, $Z = 4$; $\Delta\Lambda$-[**1**]$Cl_4\cdot3H_2O$, orthorhombic, space group *Pbca* with $a = 14.872(3)$ Å, $b = 14.533(3)$ Å, $c = 14.347(2)$ Å, $V = 3100(1)$ Å^3, $Z = 4$; $\Delta\Lambda_D$-[**4**]$Cl_2\cdot6H_2O$, monoclinic, space group $P2_1$ with $a = 7.3836(2)$ Å, $b = 20.214(1)$ Å, $c = 10.622(2)$ Å, $\beta = 91.45(1)°$ $V = 1682.0(4)$ Å^3, $Z = 2$.

Introduction

Certain thiolato groups coordinated to one Co^{III} ion tend to bind with another metal ion to form S-bridged polynuclear structures, owing to the high nucleophilic character.[1−22] Utilizing this property, a large number of S-bridged polynuclear complexes composed of [Co(thiolato-*S*)$_3$(amine-*N*)$_3$]-type octahedral units have been prepared by the reactions of *fac*(*S*)-$[Co(aet)_3]$ (aet = 2-aminoethanethiolate) or *fac*(*S*)-[Co(L-cys-*N*,*S*)$_3$]$^{3-}$ (L-cys = L-cysteinate) with a variety of metal ions.[11−22] On the other hand, S-bridged polynuclear complexes composed of [Co(thiolato-*S*)$_2$(amine-*N*)$_4$]$^+$-type units have remained largely unexplored, mainly because of

---

* Author to whom correspondence should be addressed. E-mail: konno@ch.wani.osaka-u.ac.jp.

[†] Osaka University.

[‡] Gunma University.

(1) Lane, R. H.; Pantaleo, N. S.; Farr, J. K.; Coney, W. M.; Newton, M. G. *J. Am. Chem. Soc.* **1978**, *100*, 1610.

(2) Heeg, M. J.; Elder, R. C.; Deutsch, E. *Inorg. Chem.* **1979**, *18*, 2036.

(3) Heeg, M. J.; Elder, R. C.; Deutsch, E. *Inorg. Chem.* **1980**, *19*, 554.

(4) Suades, J.; Solans, X.; F-Altaba, M.; Aguilo, M. *Inorg. Chim. Acta* **1985**, *99*, 1.

(5) Beissel, T.; Birkelbach, F.; Bill, E.; Glaser, T.; Kesting, F.; Krebs, C.; Weyhermuller, T.; Wieghardt, K.; Butzlaff, C.; Trautwein, A. X. *J. Am. Chem. Soc.* **1996**, *118*, 12376.

(6) Krebs, C.; Glaser, T.; Bill, E.; Weyhermuller, T.; M-Klaucke, W.; Wieghardt, K. *Angew. Chem., Int. Ed.* **1999**, *38*, 359.

10.1021/ic010696c CCC: $22.00

the difficulty in isolation of this type mononuclear species,[23−26] and thus the key to control their structures and chiral properties has not been clarified.

Recently, we have reported that a linear-type S-bridged $\mathrm{Co^{III}Ni^{II}Co^{III}}$ trinuclear complex, $[\mathrm{Ni}\{\mathrm{Co(aet)_2(en)}\}_2]^{4+}$, which is easily prepared from $[\mathrm{CoCl_2(en)_2}]\mathrm{Cl}$ and $[\mathrm{Ni(aet)_2}]$,[27] reacts with $[\mathrm{PdCl_4}]^{2-}$ to give S-bridged $\mathrm{Co^{III}Pd^{II}}$ dinuclear and $\mathrm{Co^{III}Pd^{II}Co^{III}}$ trinuclear complexes composed of C_2-*cis*(*S*)-$[\mathrm{Co(aet)_2(en)}]^{+}$ units, $[\mathrm{PdCl_2}\{\mathrm{Co(aet)_2(en)}\}]^{+}$ and $[\mathrm{Pd}\{\mathrm{Co(aet)_2(en)}\}_2]^{4+}$, depending on the reaction stoichiometry.[28] Furthermore, $[\mathrm{PdCl_2}\{\mathrm{Co(aet)_2(en)}\}]^{+}$ was found to be convertible to $[\mathrm{Pd}\{\mathrm{Co(aet)_2(en)}\}_2]^{4+}$ by treatment with $[\mathrm{Ni}\{\mathrm{Co(aet)_2(en)}\}_2]^{4+}$. From these results it was evidenced that $[\mathrm{Ni}\{\mathrm{Co(aet)_2(en)}\}_2]^{4+}$ acts as a donor of the *cis*(*S*)-$[\mathrm{Co(aet)_2(en)}]^{+}$ unit available for the construction of S-bridged polynuclear structures and that the $\mathrm{Cl^-}$ ions in $[\mathrm{PdCl_2}\{\mathrm{Co(aet)_2(en)}\}]^{+}$ can be replaced by two S atoms of the *cis*(*S*)-$[\mathrm{Co(aet)_2(en)}]^{+}$ unit. Of two possible forms, meso ($\Delta\Lambda$) and racemic ($\Delta\Delta/\Lambda\Lambda$), only the racemic form was produced for $[\mathrm{Pd}\{\mathrm{Co(aet)_2(en)}\}_2]^{4+}$, as in the case of the starting complex $[\mathrm{Ni}\{\mathrm{Co(aet)_2(en)}\}_2]^{4+}$. This is wholly in contrast to the fact that the S-bridged trinuclear complexes composed of tris(thiolato)-type *fac*(*S*)-$[\mathrm{Co(aet)_3}]$ units, $[\mathrm{M}\{\mathrm{Co(aet)_3}\}_2]^{3+}$ (M = $\mathrm{Co^{III}}$, $\mathrm{Fe^{III}}$), give both the meso and racemic forms.[11,12] We, therefore, examined the reaction of the racemic Δ/Λ-$[\mathrm{PdCl_2}\{\mathrm{Co(aet)_2(en)}\}]^{+}$ with the Λ_D configurational *trans*(*N*)-$[\mathrm{Co}(\text{D-pen-}N,O,S)_2]^{-}$ (D-pen = D-penicillaminate),[29] expecting the chiral selective formation of $\Lambda\Lambda_\mathrm{D}$-$[\mathrm{Pd}\{\mathrm{Co(aet)_2(en)}\}\{\mathrm{Co}(\text{D-pen-}N,O,S)_2\}]^{2+}$. As expected, it was found that only the $\Lambda\Lambda_\mathrm{D}$ isomer was formed for $[\mathrm{Pd}\{\mathrm{Co(aet)_2(en)}\}\{\mathrm{Co}(\text{D-pen-}N,O,S)_2\}]^{2+}$. However, this reaction was found to produce $\Delta\Delta$-$[\mathrm{Pd}\{\mathrm{Co(aet)_2(en)}\}_2]^{4+}$ and $\Lambda_\mathrm{D}\Lambda_\mathrm{D}$-$[\mathrm{Pd}\{\mathrm{Co}(\text{D-pen-}N,O,S)_2\}_2]^{0}$, besides $\Lambda\Lambda_\mathrm{D}$-$[\mathrm{Pd}\{\mathrm{Co(aet)_2(en)}\}\{\mathrm{Co}(\text{D-pen-}N,O,S)_2\}]^{2+}$, in a ratio of 1:1:2, which suggested that metathesis occurs between Δ-$[\mathrm{PdCl_2}\{\mathrm{Co(aet)_2(en)}\}]^{+}$ and *trans*(*N*)-$[\mathrm{Co}(\text{D-pen-}N,O,S)_2]^{-}$, because of the cleavage of the Pd−S bonds.

In these circumstances, it is worthwhile to investigate the stereochemical behavior of the linear-type S-bridged $\mathrm{Co^{III}MCo^{III}}$ trinuclear system composed of *cis*(*S*)-$[\mathrm{Co(aet)_2(en)}]^{+}$ and/or *trans*(*N*)-$[\mathrm{Co}(\text{D-pen-}N,O,S)_2]^{-}$ units, introducing a square-planar $\mathrm{Pt^{II}}$ ion at the center of the trinuclear structure, which commonly forms stronger bonds with coordinated thiolato groups. In this paper we report on the synthesis, characterization, and chiral properties of the S-bridged $\mathrm{Co^{III}Pt^{II}Co^{III}}$ trinuclear complexes, $[\mathrm{Pt}\{\mathrm{Co(aet)_2(en)}\}_2]^{4+}$ ($[\mathbf{1}]^{4+}$), $[\mathrm{Pt}\{\mathrm{Co}(\text{D-pen-}N,O,S)_2\}_2]^{0}$ ($[\mathbf{3}]$), and $[\mathrm{Pt}\{\mathrm{Co(aet)_2(en)}\}\{\mathrm{Co}(\text{D-pen-}N,O,S)_2\}]^{2+}$ ($[\mathbf{4}]^{2+}$). The crystal structures of the meso-type isomers, $\Delta\Lambda$-$[\mathbf{1}]^{4+}$ and $\Delta\Lambda_\mathrm{D}$-$[\mathbf{4}]^{2+}$, which have not been obtained for the corresponding $\mathrm{Co^{III}Pd^{II}Co^{III}}$ complexes, along with the structure of $\Delta\Delta/\Lambda\Lambda$-$[\mathbf{1}]^{4+}$, are also presented. It is anticipated that the systematic investigation of this relatively basic trinuclear system will contribute significantly not only to our understanding of the coordination chemistry of S-bridged polynuclear complexes but also to the development of chiral selective construction of polynuclear systems.

Experimental Section

Preparation, Separation, and Optical Resolution of $[\mathrm{Pt}\{\mathrm{Co(aet)_2(en)}\}_2]\mathrm{Cl_4}$ ($[\mathbf{1}]\mathrm{Cl_4}$). To a dark brown solution of $\Delta\Delta/\Lambda\Lambda$-$[\mathrm{Ni}\{\mathrm{Co(aet)_2(en)}\}_2]\mathrm{Cl_4}\cdot 6\mathrm{H_2O}$ [27b] (0.41 g, 0.48 mmol) in 140 $\mathrm{cm^3}$ of water was added a solution containing 0.20 g (0.48 mmol) of $\mathrm{K_2[PtCl_4]}$ in 40 $\mathrm{cm^3}$ of water. The mixture was stirred at 60 °C for 40 min, which gave a dark red-brown solution. The reaction solution was poured onto an SP-Sephadex C-25 cation-exchange column ($\mathrm{Na^+}$ form, 4.5 cm × 45 cm). After the column had been washed with water, two red-brown bands of $[\mathbf{1a}]^{4+}$ ($\Delta\Delta/\Lambda\Lambda$-$[\mathbf{1}]^{4+}$) and $[\mathbf{1b}]^{4+}$ ($\Delta\Lambda$-$[\mathbf{1}]^{4+}$) were eluted in this order with a 0.5 mol $\mathrm{dm^{-3}}$ aqueous solution of NaCl. The formation ratio of $[\mathbf{1a}]^{4+}$:$[\mathbf{1b}]^{4+}$ for this reaction was estimated to be ca. 1.2:1, based on the absorption spectral measurements. Each eluate of the two bands was concentrated to a small volume with a rotary evaporator. After removal of deposited NaCl by filtration, the filtrate was allowed to stand at room temperature overnight. The resulting red-brown microcrystals were collected by filtration and then recrystallized from water at room temperature. Yield for $[\mathbf{1a}]\mathrm{Cl_4}\cdot 6\mathrm{H_2O}$: 0.18 g. Anal. Calcd for $[\mathrm{Pt}\{\mathrm{Co(aet)_2(en)}\}_2]\mathrm{Cl_4}\cdot 6\mathrm{H_2O}$: C, 14.59; H, 5.31; N, 11.35. Found: C, 14.57; H, 5.36; N, 11.09. $^{13}\mathrm{C}$ NMR ($\mathrm{D_2O}$): δ 36.37 ($-\mathrm{CH_2S}$ of aet), 46.57 ($-\mathrm{CH_2NH_2}$ of en), 54.96 ($-\mathrm{CH_2NH_2}$ of aet). Yield for $[\mathbf{1b}]\mathrm{Cl_4}\cdot 3\mathrm{H_2O}$: 0.09 g. Anal. Calcd for $[\mathrm{Pt}\{\mathrm{Co(aet)_2(en)}\}_2]\mathrm{Cl_4}\cdot 3\mathrm{H_2O}$: C, 15.44; H, 4.97; N, 12.01. Found: C, 15.53; H, 5.06;

---

(7) Tokuda, K.; Okamoto, K.; Konnno, T. *Inorg. Chem.* **2000**, *39*, 333.

(8) Konno, T.; Hattori, M.; Yoshimura, T.; Hirotsu, M.*Chem. Lett.* **2000**, 852.

(9) Konno, T.; Tokuda, K.; Okamoto, K.; Hirotsu, M. *Chem. Lett.* **2000**, 1258.

(10) Konno, T.; Yoshimura, T.; Aoki, K.; Okamoto, K.; Hirotsu, M. *Angew. Chem., Int. Ed.* **2001**, *40*, 1765.

(11) (a) Busch, D. H.; Jicha, D. C. *Inorg. Chem.* **1962**, *1*, 884. (b) Brubaker, G. R.; Douglas, B. E. *Inorg. Chem.* **1967**, *6*, 1562. (c) Konno, T.; Okamoto, K.; Hidaka, J. *Acta Crystallogr.* **1993**, *C49*, 222.

(12) DeSimone, R. E.; Ontko, T.; Wardman, L.; Blinn, E. L. *Inorg. Chem.* **1975**, *14*, 1313.

(13) Blinn, E. L.; Butler, P.; Chapman, K. M.; Harris, S. *Inorg. Chim. Acta* **1977**, *24*, 139.

(14) (a) Konno, T.; Aizawa, S.; Okamoto, K.; Hidaka, J. *Chem. Lett.* **1985**, 1017. (b) Okamoto, K.; Aizawa, S.; Konno, T.; Einaga, H.; Hidaka, J. *Bull. Chem. Soc. Jpn.* **1986**, *59*, 3859.

(15) Johnson, D. W.; Brewer, T. R. *Inorg. Chim. Acta* **1988**, *151*, 221.

(16) Konno, T.; Okamoto, K.; Hidaka, J. *Bull. Chem. Soc. Jpn.* **1990**, *63*, 3027.

(17) Okamoto, K.; Yonemura, T.; Konno, T.; Hidaka, J. *Bull. Chem. Soc. Jpn.* **1992**, *65*, 794.

(18) Konno, T.; Nagashio, T.; Okamoto, K.; Hidaka, J. *Inorg. Chem.* **1992**, *31*, 1160.

(19) (a) Kageyama, Y.; Konno, T.; Okamoto, K.; Hidaka, J. *Inorg. Chim. Acta* **1995**, *239*, 19. (b) Okamoto, K.; Kageyama, Y.; Konno, T. *Bull. Chem. Soc. Jpn.* **1995**, *68*, 2573.

(20) Konno, T.; Tokuda, K.; Suzuki, T.; Okamoto, K. *Bull. Chem. Soc. Jpn.* **1998**, *71*, 1049.

(21) Okamoto, K.; Sasaki, C.; Yamada, Y.; Konno, T. *Bull. Chem. Soc. Jpn.* **1999**, *72*, 1685.

(22) Konno, T.; Chikamoto, Y.; Okamoto, K.; Yamaguchi, T.; Ito, T.; Hirotsu, M. *Angew. Chem., Int. Ed.* **2000**, *39*, 4098.

(23) Stein, C.; Bouma, S.; Carlson, J.; Cornelius, C.; Maeda, J.; Weschler, C.; Deutsch, E.; Hodgson, K. O. *Inorg. Chem.* **1976**, *15*, 1976.

(24) Yamanari, K.; Takeshita, N.; Shimura, Y. *Bull. Chem. Soc. Jpn.* **1984**, *57*, 1227.

(25) Yamanari, K.; Takeshita, N.; Shimura, Y. *Bull. Chem. Soc. Jpn.* **1984**, *57*, 2852.

(26) Yonemura, T.; Bai, Z.-P.; Okamoto, K.; Ama, T.; Kawaguchi, H.; Yasui, T.; Hidaka, J. *J. Chem. Soc., Dalton Trans.* **1999**, 2151.

(27) (a) Konno, T.; Okamoto, K.; Hidaka, J. *Inorg. Chem.* **1992**, *31*, 160. (b) Konno, T.; Hidaka, J.; Okamoto, K. *Bull. Chem. Soc. Jpn.* **1995**, *68*, 1353.

(28) Konno, T.; Machida, T.; Okamoto, K. *Bull. Chem. Soc. Jpn.* **1998**, *71*, 175.

(29) Konno, T.; Matsuno, N.; Okamoto, K.; Hirotsu, M. *Chem. Lett.* **1999**, 1243.

N, 11.90. ^{13}C NMR (D_2O): δ 37.39 ($-CH_2S$ of aet), 46.52 ($-CH_2NH_2$ of en), 54.55 ($-CH_2NH_2$ of aet).

An aqueous solution of [**1a**]$Cl_4 \cdot 6H_2O$ was chromatographed on an SP-Sephadex C-25 column (Na^+ form, 4.5 cm × 45 cm), using a 0.25 mol dm^{-3} aqueous solution of $Na_2[Sb_2(R,R\text{-tartrato})_2] \cdot 5H_2O$ as an eluent. When the developed band was completely separated into two bands in the column, the eluent was changed to a 0.5 mol dm^{-3} aqueous solution of $NaClO_4$. Each eluate of the two bands was concentrated to a small volume with a rotary evaporator, and the concentrated solution was used for the CD spectral measurement. The concentration of each eluate was evaluated on the basis of the absorption spectral data of the racemic salt [**1a**]$Cl_4 \cdot 6H_2O$. It was found from the CD spectral measurements that the earlier and the later moving bands in the column contained the $(+)^{CD}_{520}$ and $(-)^{CD}_{520}$ isomers, respectively.

Preparation of $[PtCl_2\{Co(aet)_2(en)\}]Cl$ ([2]Cl). To a solution containing 0.71 g (0.83 mmol) of $[Ni\{Co(aet)_2(en)\}_2]Cl_4 \cdot 6H_2O$[27b] in 70 cm^3 of water was added a solution containing 0.70 g (1.69 mmol) of $K_2[PtCl_4]$ in 140 cm^3 of warm water. The mixture was stirred at 80 °C for 30 min, which gave a red-brown solution. After removal of a trace amount of orange powder by filtration, the filtrate was concentrated to ca. 80 cm^3 with a rotary evaporator, which was allowed to stand at room temperature for 6 days. The resulting dark red-brown crystals were collected by filtration. Yield: 0.51 g. Anal. Calcd for $[PtCl_2\{Co(aet)_2(en)\}]Cl \cdot H_2O$: C, 12.19; H, 3.75; N, 9.49. Found: C, 12.37; H, 3.67; N, 9.43. ^{13}C NMR (D_2O): δ 36.53 ($-CH_2S$ of aet), 46.49 ($-CH_2NH_2$ of en), 53.29 ($-CH_2NH_2$ of aet).

Preparation of $\Lambda_D\Lambda_D$-$[Pt\{Co(\text{D-pen-}N,O,S)_2\}_2]^0$ ($\Lambda_D\Lambda_D$-[3]). To a solution containing 0.07 g (0.16 mmol) of Λ_D-*trans*(*N*)-K[Co(D-pen-*N*,*O*,*S*)$_2$]$\cdot 2.5H_2O$[30] in 20 cm^3 of water was added 0.05 g (0.12 mmol) of $K_2[PtCl_4]$ in 10 cm^3 of water. The mixture was stirred at 60 °C for 1 h, during which time the color of the solution changed from dark brown to dark green. The reaction solution was allowed to stand at room temperature for 7 days, and then the resulting green microcrystals were collected by filtration. Yield: 0.039 g. Anal. Calcd for $[Pt\{Co(\text{D-pen})_2\}_2] \cdot 6H_2O$: C, 23.79; H, 4.79; N, 5.55. Found: C, 23.86; H, 4.82; N, 5.53. ^{13}C NMR (D_2O): δ 30.75 ($-CH_3$), 35.57 ($-CH_3$), 54.74 ($-CS$), 75.55 ($-CHNH_2$), 183.32 ($-COO$).

Preparation and Separation of $[Pt\{Co(aet)_2(en)\}\{Co(\text{D-pen-}N,O,S)_2\}]Cl_2$ ([4]Cl_2). To a solution containing 0.50 g (0.85 mmol) of [**2**]$Cl \cdot H_2O$ in 600 cm^3 of warm water was added a solution containing 0.45 g (1.02 mmol) of Λ_D-*trans*(*N*)-K[Co(D-pen-*N*,*O*,*S*)$_2$]$\cdot 2.5H_2O$[30] in 100 cm^3 of water. The mixture was stirred at 60 °C for 30 min, which gave a deep red-brown solution. The reaction solution was poured onto an SP-Sephadex C-25 column (Na^+ form, 4.5 cm × 70 cm). A pale yellow-brown band containing $\Lambda_D\Lambda_D$-[**3**] and unreacted Λ_D-*trans*(*N*)-[Co(D-pen-*N*,*O*,*S*)$_2$]$^-$ was eluted with water, two dark brown bands of [**4a**]$^{2+}$ ($\Lambda\Lambda_D$-[**4**]$^{2+}$) and [**4b**]$^{2+}$ ($\Delta\Lambda_D$-[**4**]$^{2+}$) and a brown band of [**4c**]$^{2+}$ ($\Delta\Delta_D$-[**4′**]$^{2+}$) were eluted with a 0.15 mol dm^{-3} aqueous solution of NaCl, and finally two pale red-brown bands of $\Delta\Delta$-[**1**]$^{4+}$ and $\Delta\Lambda$-[**1**]$^{4+}$ were eluted with a 0.5 mol dm^{-3} aqueous solution of NaCl. Complex $\Lambda_D\Lambda_D$-[**3**] was separated from Λ_D-*trans*(*N*)-[Co(D-pen-*N*,*O*,*S*)$_2$]$^-$ by QAE-Sephadex A-25 anion-exchange column (Cl^- form, 4.5 cm × 45 cm); a dark green band of $\Lambda_D\Lambda_D$-[**3**] was eluted with water, while Λ_D-*trans*(*N*)-[Co(D-pen-*N*,*O*,*S*)$_2$]$^-$ was adsorbed on the top of the column. The formation ratio of $\Delta\Delta$-[**1**]$^{4+}$:$\Delta\Lambda$-[**1**]$^{4+}$:$\Lambda_D\Lambda_D$-[**3**]:[**4a**]$^{2+}$:[**4b**]$^{2+}$:[**4c**]$^{2+}$ for this reaction was estimated to be ca. 0.1:0.1:0.2:8:5:1, based on the absorption spectral measurements. Each eluate of the [**4a**]$^{2+}$ and [**4b**]$^{2+}$ bands was concentrated to a small volume with a rotary evaporator. After removal of deposited NaCl by filtration, the filtrate was concentrated to dryness with a rotary evaporator. The residue was suspended in an appropriate amount of methanol, followed by the addition of a minimum amount of water to dissolve contaminated NaCl. The remaining brown powder was collected by filtration and then recrystallized from water at room temperature. Yield for [**4a**]$Cl_2 \cdot 2.5H_2O$: 0.10 g. Anal. Calcd for $[Pt\{Co(aet)_2(en)\}\{Co(\text{D-pen})_2\}]Cl_2 \cdot 2.5H_2O$: C, 20.54; H, 4.63; N, 8.90. Found: C, 20.54; H, 4.66; N, 8.93. ^{13}C NMR (D_2O): δ 30.99 ($-CH_3$ of pen), 34.68 ($-CH_3$ of pen), 36.49 ($-CH_2S$ of aet), 46.52 ($-CH_2NH_2$ of en), 54.01 ($-CS$ of pen), 54.89 ($-CH_2NH_2$ of aet), 75.70 ($-CHNH_2$ of pen), 183.46 ($-COO$ of pen). Yield for [**4b**]$Cl_2 \cdot 6H_2O$: 0.05 g. Anal. Calcd for $[Pt\{Co(aet)_2(en)\}\{Co(\text{D-pen})_2\}]Cl_2 \cdot 6H_2O$: C, 19.24; H, 5.05; N, 8.41. Found: C, 18.94; H, 5.10; N, 8.25. ^{13}C NMR (D_2O): δ 30.62 ($-CH_3$ of pen), 34.67 ($-CH_3$ of pen), 37.15 ($-CH_2S$ of aet), 46.52 ($-CH_2NH_2$ of en), 53.80 ($-CS$ of pen), 55.82 ($-CH_2NH_2$ of aet), 76.26 ($-CHNH_2$ of pen), 183.46 ($-COO$ of pen).

Table 1. Crystallographic Data for $\Delta\Delta/\Lambda\Lambda$-[**1**]$Cl_4 \cdot 6H_2O$, $\Delta\Lambda$-[**1**]$Cl_4 \cdot 3H_2O$, and $\Delta\Lambda_D$-[**4**]$Cl_2 \cdot 6H_2O$

	$\Delta\Delta/\Lambda\Lambda$-[**1**]$Cl_4 \cdot 6H_2O$	$\Delta\Lambda$-[**1**]$Cl_4 \cdot 3H_2O$	$\Delta\Lambda_D$-[**4**]$Cl_2 \cdot 6H_2O$
empirical formula	$C_{12}H_{52}Cl_4Co_2N_8O_6PtS_4$	$C_{12}H_{46}Cl_4Co_2N_8O_3PtS_4$	$C_{16}H_{50}Cl_2Co_2N_6O_{10}PtS_4$
fw	987.60	933.56	998.71
cryst syst	monoclinic	orthorhombic	monoclinic
space group	*C*2/*c* (No. 15)	*Pbca* (No. 61)	$P2_1$ (No. 4)
T, K	296	293	291
a, Å	14.983(3)	14.872(3)	7.836(2)
b, Å	19.857(4)	14.533(3)	20.214(1)
c, Å	12.949(3)	14.347(2)	10.622(2)
β, deg	113.51(2)		91.45(1)
V, Å^3	3532(1)	3100(1)	1682.0(4)
Z	4	4	2
ρ_{calcd}, g cm^{-3}	1.857	2.038	1.972
μ(Mo Kα), cm^{-1}	54.40	61.84	55.68
R^a	0.038	0.059	0.037
$R_w{}^b$	0.044	0.060	0.040

[a] $R = \sum|(|F_o| - |F_c|)|/\sum(|F_o|)$. [b] $R_w = [\sum w(|F_o| - |F_c|)^2/\sum w(|F_o|)^2]^{1/2}$, $w = 1/\sigma^2(F_o)$.

Isolation of the compound from the [**4c**]$^{2+}$ eluate was also attempted by the same procedure described above. However, no significant amount of solid was obtained, because of the low formation ratio and the high solubility in water. Thus, the absorption and CD spectra for [**4c**]$^{2+}$ were measured only qualitatively.

Physical Measurements. The electronic absorption spectra were recorded with a JASCO Ubset-55 spectrophotometer, and the CD spectra were recorded with a JASCO J-700 spectropolarimeter in aqueous solutions at room temperature. The ^{13}C NMR spectra were recorded with a JEOL JNM-A500 NMR spectrometer in D_2O at the probe temperature. Sodium 4,4-dimethyl-4-silapentane-1-sulfonate (DSS) was used as the internal reference. The elemental analyses (C, H, N) were performed by the Analysis Center of the University of Tsukuba. The concentrations of Co and Pt in the complexes were determined by plasma emission spectral analyses with a SHIMADZU ICP-1000III ICP spectrometer. The molar conductivities were measured with a Horiba DS-12 conductivity meter in water at room temperature.

X-ray Structural Determinations. Single-crystal X-ray diffraction experiments for [**1a**]$Cl_4 \cdot 6H_2O$, [**1b**]$Cl_4 \cdot 3H_2O$, and [**4b**]$Cl_2 \cdot 6H_2O$ were performed on a Rigaku AFC-7S diffractometer with a graphite-monochromatized Mo Kα radiation (λ = 0.71073 Å). Crystallographic data are summarized in Table 1. Unit-cell param-

---

(30) Okamoto, K.; Wakayama, K.; Einaga, E.; Yamada, S.; Hidaka, J. *Bull. Chem. Soc. Jpn.* **1983**, *56*, 165.

eters were determined by a least-squares refinement, using the setting angles of 25 reflections (25° $\leq 2\theta \leq$ 30°). The intensity data were collected by the $\omega{-}2\theta$ scan mode up to 55°. The intensities were corrected for Lorentz and polarization. Empirical absorption corrections based on a series of ψ scans were also applied. The 3210, 1601, and 3573 independent reflections with $I > 2.0\sigma(I)$ of the measured 4067, 3988, and 3990 reflections were considered as "observed" and used for structure determinations of [**1a**]Cl_4·$6H_2O$, [**1b**]Cl_4·$3H_2O$, and [**4b**]Cl_2·$6H_2O$, respectively.

The positions of Co, Pt, and S atoms for [**1a**]Cl_4·$6H_2O$ and [**4b**]Cl_2·$6H_2O$ were determined by direct methods, while those for [**1b**]Cl_4·$3H_2O$ were determined by the Patterson method. The remaining non-H atoms were found by successive difference Fourier techniques. The structures were refined by full-matrix least-squares techniques using anisotropic thermal parameters for non-H atoms. All H atoms, except for water H atoms, were located and added to calculations but not refined. All calculations were performed using the teXsan crystallographic software package.[31]

Results and Discussion

Synthesis and Characterization of [1]$^{4+}$, [2]$^+$, and [3]. Treatment of a dark brown aqueous solution of $[Ni\{Co(aet)_2(en)\}_2]Cl_4$ with 1 molar equiv of $K_2[PtCl_4]$ gave a dark red-brown solution, which was found to contain [**1a**]$^{4+}$ and [**1b**]$^{4+}$ in a ratio of ca. 1.2:1. Complexes [**1a**]$^{4+}$ and [**1b**]$^{4+}$ were separated by SP-Sephadex C-25 column chromatography and then isolated as the chloride salts. The plasma emission spectral analyses (Pt/Co = 0.53 for [**1a**]$^{4+}$ and 0.54 for [**1b**]$^{4+}$) indicated that each complex contains Co and Pt atoms in a ratio of 2:1, and their elemental analytical results are consistent with the expected S-bridged $Co^{III}Pt^{II}Co^{III}$ trinuclear structure in $[Pt\{Co(aet)_2(en)\}_2]Cl_4$. The crystal structure of each complex was determined by X-ray crystallography, which demonstrated that [**1a**]$^{4+}$ and [**1b**]$^{4+}$ are the racemic ($\Delta\Delta/\Lambda\Lambda$) and meso ($\Delta\Lambda$) forms of $[Pt\{Co(aet)_2(en)\}_2]^{4+}$, respectively (vide infra). It is noteworthy that this is the first example of the isolation of the two forms for the S-bridged trinuclear complexes of this class; only the racemic form has been obtained for $[Ni\{Co(aet)_2(en)\}_2]^{4+}$,[27] $[Pd\{Co(aet)_2(en)\}_2]^{4+}$,[28] and $[CdCl\{Co(aet)_2(en)\}_2]^{3+}$.[32] In the ^{13}C NMR spectrum each of $\Delta\Delta/\Lambda\Lambda$-[**1**]$^{4+}$ and $\Delta\Lambda$-[**1**]$^{4+}$ exhibits three sharp signals for the 12 methylene carbon atoms in the complex; the signals for $\Delta\Delta/\Lambda\Lambda$-[**1**]$^{4+}$ appear at δ 36.37, 46.57, and 54.96, while those for $\Delta\Lambda$-[**1**]$^{4+}$ appear at δ 37.39, 46.52, and 54.55. This implies that the S-bridged trinuclear structures of $\Delta\Delta/\Lambda\Lambda$-[**1**]$^{4+}$ (idealized D_2 symmetry) and $\Delta\Lambda$-[**1**]$^{4+}$ (idealized C_{2h} symmetry) observed in crystal are retained in solution. As shown in Figure 1 and Table 2, the electronic absorption spectra of $\Delta\Delta/\Lambda\Lambda$-[**1**]$^{4+}$ and $\Delta\Lambda$-[**1**]$^{4+}$ are similar to each other over the whole region. In particular, the two complexes exhibit almost overlapping visible bands at ca. 20×10^3 cm^{-1}, which are assignable as arising from a d−d transition for the terminal Co^{III} centers. However, it is noticed that the absorption curves for $\Delta\Delta/\Lambda\Lambda$-[**1**]$^{4+}$ and $\Delta\Lambda$-[**1**]$^{4+}$ are slightly deviated from each other in the near-UV region of ca. 34×10^3 to 48×10^3 cm^{-1}. This suggests that the absorption spectra in this region are dominated by the central $Pt^{II}S_4$ chromophore, and therefore the difference in the $Pt^{II}S_4$ coordination environment between $\Delta\Delta/\Lambda\Lambda$-[**1**]$^{4+}$ and $\Delta\Lambda$-[**1**]$^{4+}$ is reflected in this region. Complex $\Delta\Delta/\Lambda\Lambda$-[**1**]$^{4+}$ was successfully optically resolved into the $(+)^{CD}_{520}$ and $(-)^{CD}_{520}$ isomers by SP-Sephadex C-25 column chromatography using $[Sb_2(R,R\text{-tartrato})_2]^{2-}$ as the resolving agent. The CD spectral behavior of the $(+)^{CD}_{520}$ isomer is very similar to that of $\Lambda\Lambda$-$[Pd\{Co(aet)_2(en)\}_2]^{4+}$,[28] giving two positive CD bands in the visible region of ca. 16×10^3 to 28×10^3 cm^{-1} and two negative CD bands in the near-UV region of ca. 28×10^3 to 38×10^3 cm^{-1} (Figure 2 and Table 2). Thus, the $(+)^{CD}_{520}$ isomer of [**1**]$^{4+}$ is assignable to have the $\Lambda\Lambda$ configuration, while the $(-)^{CD}_{520}$ isomer, which shows a CD spectrum enantiomeric to the spectrum of $(+)^{CD}_{520}$-[**1**]$^{4+}$, has the $\Delta\Delta$ configuration. No significant absorption and CD spectral changes with time were noticed for $\Delta\Delta$-, $\Lambda\Lambda$-, and $\Delta\Lambda$-[**1**]$^{4+}$ at least for 1 day. This result clearly implies that the intermolecular or intramolecular exchange of the two C_2-

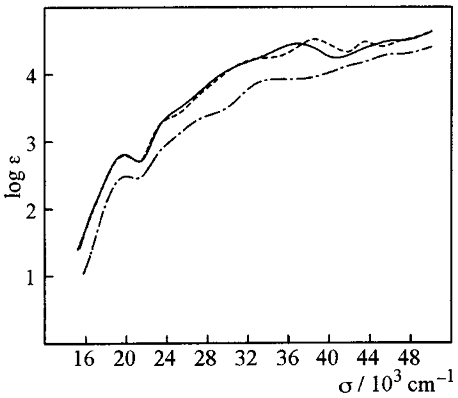

Figure 1. Absorption spectra of [**1a**]$^{4+}$ ($\Delta\Delta/\Lambda\Lambda$-[**1**]$^{4+}$) (—), [**1b**]$^{4+}$ ($\Delta\Lambda$-[**1**]$^{4+}$) (- - -), and [**2**]$^+$ (— · —) in H_2O.

Table 2. Absorption and CD Spectral Data of $\Lambda\Lambda$-[**1**]$^{4+}$, $\Delta\Lambda$-[**1**]$^{4+}$, and [**2**]$^+$ in H_2O[a]

abs max: $\sigma/10^3$ cm^{-1} (log ϵ/mol^{-1} dm^3 cm^{-1})		CD extrema: $\sigma/10^3$ cm^{-1} ($\Delta\epsilon$/mol^{-1} dm^3 cm^{-1})	
$\Lambda\Lambda$-$[Pt\{Co(aet)_2(en)\}_2]^{4+}$ ($\Lambda\Lambda$-[**1**]$^{4+}$)			
19.81	(2.81)	19.23	(+11.98)
23.8	(3.3)^{sh}	24.01	(+23.29)
30.6	(4.4)^{sh}	30.67	(−43.51)
36.93	(4.45)	35.91	(−47.43)
45.4	(4.5)^{sh}	39.22	(+36.46)
		44.84	(+96.38)
		47.73	(+68.35)
meso-$[Pt\{Co(aet)_2(en)\}_2]^{4+}$ ($\Delta\Lambda$-[**1**]$^{4+}$)			
19.82	(2.79)		
23.8	(3.3)^{sh}		
32.0	(4.2)^{sh}		
38.49	(4.51)		
43.48	(4.46)		
47.4	(4.5)^{sh}		
$[PtCl_2\{Co(aet)_2(en)\}]^+$ ([**2**]$^+$)			
20.02	(2.49)		
23.3	(2.9)^{sh}		
27.8	(3.4)^{sh}		
35.01	(3.93)		
46.3	(4.3)^{sh}		

[a] The sh label denotes a shoulder.

---

(31) Crystal Structure Analysis Package, Molecular Structure Corporation, 1985 and 1992.

(32) Konno, T.; Tokuda, K.; Sakurai, J.; Okamoto, K. *Bull. Chem. Soc. Jpn.* **2000**, *73*, 2767.

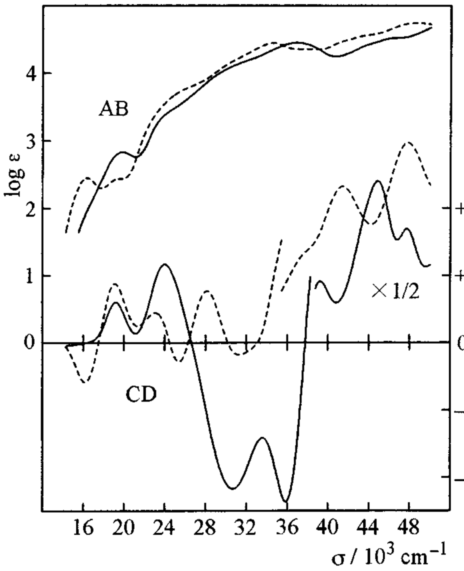

Figure 2. Absorption and CD spectra of $(+)^{CD}_{520}$-$\Lambda\Lambda$-[**1**]$^{4+}$ (—) and $\Lambda_D\Lambda_D$-[**3**] (- - -) in H_2O.

cis(*S*)-[$Co(aet)_2(en)$]$^+$ units, as well as its racemization, does not occur for [**1**]$^{4+}$, owing to the formation of the strong Pt−S bonds in the S-bridged $Co^{III}Pt^{II}Co^{III}$ trinuclear structure.

The reaction of [$Ni\{Co(aet)_2(en)\}_2$]Cl_4 with 2 molar equiv of $K_2[PtCl_4]$ in water gave a deep red-brown solution, from which [**2**]Cl·H_2O was isolated in a reasonable yield. The plasma emission spectral analysis (Pt/Co = 0.99) indicated that this complex contains Co and Pt atoms in a ratio of 1:1, and its elemental analytical result is consistent with the expected S-bridged $Co^{III}Pt^{II}$ dinuclear structure in [$PtCl_2\{Co(aet)_2(en)\}$]Cl. As shown in Figure 1, the absorption spectrum of [**2**]$^+$ is characterized by one intense near-UV absorption peak at ca. 35 × 10^3 cm^{-1}, which is accompanied by vague shoulders at the lower energy side. This absorption spectral behavior is similar to that of the $Pd^{II}Co^{III}$ dinuclear complex, [$PdCl_2\{Co(aet)_2(en)\}$]$^+$, in which Pd^{II} ion is bound by one C_2-*cis*(*S*)-[$Co(aet)_2(en)$]$^+$ unit and two Cl^- ions.[28] Furthermore, the ^{13}C NMR spectrum of [**2**]$^+$ corresponds well with that of [$PdCl_2\{Co(aet)_2(en)\}$]$^+$ (δ 36.99 ($-CH_2S$), 46.48 ($-CH_2N$ of en), and 54.35 ($-CH_2$ of aet)), giving only three sharp signals at δ 36.53, 46.49, and 53.29. From these results, it is reasonable to assign that [**2**]$^+$ has the S-bridged Pt^{II}-Co^{III} dinuclear structure in [$PtCl_2\{Co(aet)_2(en)\}$]$^+$ having a C_2-*cis*(*S*)-[$Co(aet)_2(en)$]$^+$ unit. This assignment is confirmed by the reaction of [**2**]$^+$ with Λ_D-*trans*(*N*)-[Co(D-pen-*N,O,S*)$_2$]$^-$, which led to the formation of S-bridged $Co^{III}Pt^{II}$-Co^{III} complexes composed of a mixture of C_2-*cis*(*S*)-[$Co(aet)_2(en)$]$^+$ and Λ_D-*trans*(*N*)-[Co(D-pen-*N,O,S*)$_2$]$^-$ units (vide infra).

Table 3. Absorption and CD Spectral Data of $\Lambda_D\Lambda_D$-[**3**], $\Lambda\Lambda_D$-[**4**]$^{2+}$, and $\Delta\Lambda_D$-[**4**]$^{2+}$ in H_2O[a]

abs max: $\sigma/10^3$ cm^{-1}	(log ϵ/mol^{-1} dm^3 cm^{-1})	CD extrema: $\sigma/10^3$ cm^{-1}	($\Delta\epsilon$/mol^{-1} dm^3 cm^{-1})
$\Lambda_D\Lambda_D$-[Pt{Co(D-pen-*N,O,S*)$_2$}$_2$]^0 ($\Lambda_D\Lambda_D$-[**3**])			
16.38	(2.45)	16.19	(−11.72)
19.5	(2.4)^{sh}	19.08	(+17.52)
26.7	(3.8)^{sh}	23.09	(+8.89)
31.2	(4.2)^{sh}	25.41	(+-5.71)
34.58	(4.45)	28.13	(+15.36)
41.6	(4.5)^{sh}	31.25	(−3.59)
43.9	(4.6)^{sh}	38.3	(+28.2)^{sh}
48.59	(4.75)	41.41	(+92.89)
		47.73	(+118.90)
$\Lambda\Lambda_D$-[Pt{$Co(aet)_2(en)$}{Co(D-pen-*N,O,S*)$_2$}]$^{2+}$ ($\Lambda\Lambda_D$-[**4**]$^{2+}$)			
16.20	(2.06)	15.86	(−3.77)
19.8	(2.7)^{sh}	19.19	(+13.91)
23.9	(3.4)^{sh}	23.53	(+14.41)
30.49	(4.1)^{sh}	30.77	(−25.06)
35.26	(4.40)	34.48	(−16.75)
37.65	(4.38)	39.2	(+37.4)^{sh}
43.5	(4.5)^{sh}	43.86	(+85.53)
45.8	(4.5)^{sh}	49.02	(+89.82)
$\Delta\Lambda_D$-[Pt{$Co(aet)_2(en)$}{Co(D-pen-*N,O,S*)$_2$}]$^{2+}$ ($\Delta\Lambda_D$-[**4**]$^{2+}$)			
16.05	(2.17)	15.93	(−5.31)
19.87	(2.64)	18.45	(+5.09)
23.1	(3.3)^{sh}	24.72	(−16.64)
32.2	(4.2)^{sh}	27.8	(+33.6)^{sh}
37.36	(4.47)	37.17	(+50.14)
42.4	(4.47)	44.44	(−50.32)

[a] The sh label denotes a shoulder.

When Λ_D-*trans*(*N*)-K[Co(D-pen-*N,O,S*)$_2$] was reacted with $K_2[PtCl_4]$ in a ratio of 2:1 in water, the solution color changed from dark brown to dark green, from which green microcrystals of $\Lambda_D\Lambda_D$-[**3**] were isolated. The plasma emission spectral analysis (Pt/Co = 0.54) indicated that this complex contains Co and Pt atoms in a ratio of 2:1, and its elemental analytical result is consistent with the S-bridged $Co^{III}Pt^{II}$-Co^{III} trinuclear structure in [Pt{Co(D-pen-*N,O,S*)$_2$}$_2$]^0. Furthermore, the molar conductivity of $\Lambda_D\Lambda_D$-[**3**] in water is 4.5 Ω^{-1} cm^2 mol^{-1}, which is compatible with the neutral species.[29] As compared in Figure 2, the absorption spectral behavior of $\Lambda_D\Lambda_D$-[**3**] resembles that of $\Delta\Delta/\Lambda\Lambda$-[**1**]$^{4+}$ especially in the energy region higher than ca. 24 × 10^3 cm^{-1}, suggesting the formation of an S-bridged $Co^{III}Pt^{II}Co^{III}$ trinuclear structure having a PtS_4 chromophore. In the ^{13}C NMR spectrum, $\Lambda_D\Lambda_D$-[**3**] gives five sharp signals corresponding to five carbon atoms of the D-pen ligand (δ 30.75 and 35.57 for $-CH_3$, 54.74 for $-CS$, 75.55 for $-CHNH_2$, and 183.32 for $-COO$). Five similar signals have been observed in the ^{13}C NMR spectrum of the S-bridged Co^{III}-$Pd^{II}Co^{III}$ trinuclear complex, $\Lambda_D\Lambda_D$-[Pd{Co(D-pen-*N,O,S*)$_2$}$_2$]^0 (δ 30.56 and 36.18 for $-CH_3$, 55.03 for $-CS$, 75.22 for $-CHNH_2$, and 183.48 for $-COO$), in which two Λ_D-*trans*(*N*)-[Co(D-pen-*N,O,S*)$_2$]$^-$ units are linked by a Pd^{II} ion through sulfur bridges to have an idealized D_2 symmetry.[29] Accordingly, it is confidently assigned that $\Lambda_D\Lambda_D$-[**3**] is the D_2-symmetrical S-bridged $Co^{III}Pt^{II}Co^{III}$ trinuclear complex, $\Lambda_D\Lambda_D$-[Pd{Co(D-pen-*N,O,S*)$_2$}$_2$]^0, in which the central Pt^{II} ion is coordinated by four thiolato S atoms from the two terminal Λ_D-*trans*(*N*)-[Co(D-pen-*N,O,S*)$_2$]$^-$ units. Complex $\Lambda_D\Lambda_D$-[**3**] is inherently optically active, and its CD spectrum is characterized by two positive CD components in the visible region (ca. 19 × 10^3 and 23 × 10^3 cm^{-1}) and three intense positive CD components in the near-UV region (ca. 38 × 10^3, 41 × 10^3, and 48 × 10^3 cm^{-1}) (Figure 2 and Table 3). This CD spectral characteristic corresponds with that of $\Lambda\Lambda$-[**1**]$^{4+}$, suggesting that the CD contribution due to the Λ configurational skew pair of N,S-chelate rings in $\Lambda_D\Lambda_D$-[**3**] is dominant in these regions. This is also the case for the

Scheme 1

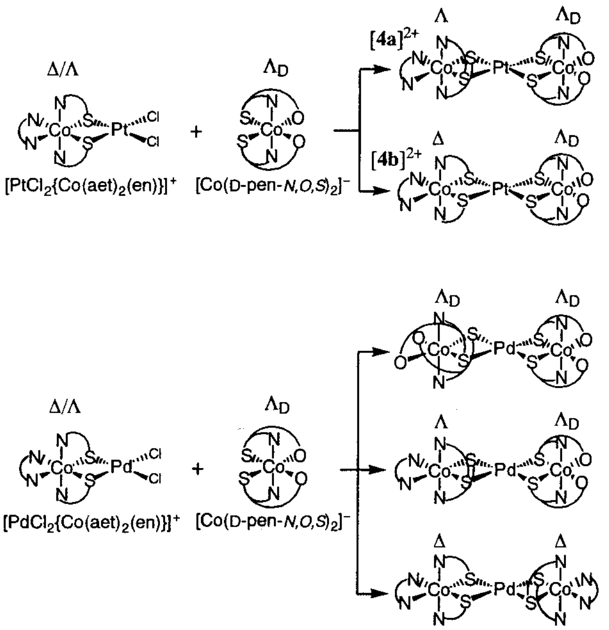

CD spectrum of Λ$_D$Λ$_D$-[Pd{Co(D-pen-*N*,*O*,*S*)$_2$}$_2$]^0, which gives CD bands quite similar to those of ΛΛ-[Pd{Co(aet)$_2$(en)}$_2$]$^{4+}$ in the visible region of ca. 17×10^3 to 26×10^3 cm^{-1} and in the near-UV region of ca. 37×10^3 to 49×10^3 cm^{-1}.[29]

Reaction of [PtCl$_2${Co(aet)$_2$(en)}]$^+$ ([2]$^+$) with Λ$_D$-*trans*(*N*)-[Co(D-pen-*N*,*O*,*S*)$_2$]$^-$. The 1:1 reaction of [**2**]Cl with Λ$_D$-*trans*(*N*)-K[Co(D-pen-*N*,*O*,*S*)$_2$] in water produced a deep red-brown solution, which was poured onto an SP-Sephadex C-25 column. When the column was washed with water, a pale yellow-brown band containing Λ$_D$Λ$_D$-[Pt{Co(D-pen-*N*,*O*,*S*)$_2$}$_2$]^0 (Λ$_D$Λ$_D$-[**3**]) and unreacted Λ$_D$-*trans*(*N*)-[Co(D-pen-*N*,*O*,*S*)$_2$]$^-$ was eluted. The adsorbed band on the top of the column was then eluted with a 0.15 mol dm^{-3} aqueous solution of NaCl, which gave three well-separated bands [**4a**]$^{2+}$ (dark-brown), [**4b**]$^{2+}$ (dark-brown), and [**4c**]$^{2+}$ (brown) in this order. Finally, two pale red-brown bands of ΔΔ-[**1**]$^{4+}$ and ΔΛ-[**1**]$^{4+}$ were eluted with a 0.5 mol dm^{-3} aqueous solution of NaCl. The formation ratio of ΔΔ-[**1**]$^{4+}$:ΔΛ-[**1**]$^{4+}$:Λ$_D$Λ$_D$-[**3**]:[**4a**]$^{2+}$:[**4b**]$^{2+}$:[**4c**]$^{2+}$ was evaluated to be ca. 0.1:0.1:0.2:8:5:1, indicating that [**4a**]$^{2+}$ and [**4b**]$^{2+}$ are the main products of this reaction (Scheme 1). Complexes [**4a**]$^{2+}$ and [**4b**]$^{2+}$ were isolated as the chloride salts, while attempts to isolate the minor product of [**4c**]$^{2+}$ were unsuccessful. It was found from the plasma emission spectral analyses (Pt/Co = 0.50 for [**4a**]$^{2+}$, 0.47 for [**4b**]$^{2+}$, and 0.47 for [**4c**]$^{2+}$) that each of the [**4a**]$^{2+}$, [**4b**]$^{2+}$, and [**4c**]$^{2+}$ eluates contains Co and Pt atoms in a ratio of 2:1.

The elemental analytical results of the isolated [**4a**]Cl$_2$ and [**4b**]Cl$_2$ are consistent with the formula for [Pt{Co(aet)$_2$(en)}{Co(D-pen-*N*,*O*,*S*)$_2$}]Cl$_2$, and X-ray analysis demonstrated that [**4b**]$^{2+}$ is the ΔΛ$_D$ isomer of [Pt{Co(aet)$_2$(en)}{Co(D-pen-*N*,*O*,*S*)$_2$}]$^{2+}$ (ΔΛ$_D$-[**4**]$^{2+}$) having an averaged C_2 symmetry (vide infra). In the ^{13}C NMR spectrum, [**4b**]$^{2+}$ exhibits five signals (*δ* 30.62, 34.67, 53.80, 76.26, and 183.46) due to the Λ$_D$-*trans*(*N*)-[Co(D-pen-*N*,*O*,*S*)$_2$]$^-$ unit and three signals (*δ* 37.15, 46.52, and 55.82) due to the Δ-C_2-*cis*(*S*)-[Co(aet)$_2$(en)]$^+$ unit. A very similar ^{13}C NMR spectrum was observed for [**4a**]$^{2+}$, which gives the five corresponding signals at *δ* 30.99, 34.68, 54.01, 75.70, and 183.46, together with the three signals at *δ* 36.49, 46.52, and 54.89. This NMR spectrum indicates that [**4b**]$^{2+}$ also has the Co^{III}Pt^{II}Co^{III} trinuclear structure composed of the C_2-*cis*(*S*)-[Co(aet)$_2$(en)]$^+$ and Λ$_D$-*trans*(*N*)-[Co(D-pen-*N*,*O*,*S*)$_2$]$^-$ units. Consistent with this assignment, the absorption spectral behavior of [**4a**]$^{2+}$ coincides well with that of [**4b**]$^{2+}$ over the whole region, as illustrated in Figure 3. However, the CD spectrum of [**4a**]$^{2+}$ is markedly different from that of [**4b**]$^{2+}$, especially in the energy region higher than ca. 22×10^3 cm^{-1} (Figure 3 and Table 3), and its overall spectral feature resembles that of ΛΛ-[Pt{Co(aet)$_2$(en)}$_2$]$^{4+}$ (ΛΛ-[**1**]$^{4+}$) (Figure 2). Accordingly, it is undoubtedly assigned that [**4a**]$^{2+}$ is the ΛΛ$_D$ isomer of [Pt{Co(aet)$_2$(en)}{Co(D-pen-*N*,*O*,*S*)$_2$}]$^{2+}$ (ΛΛ$_D$-[**4**]$^{2+}$).

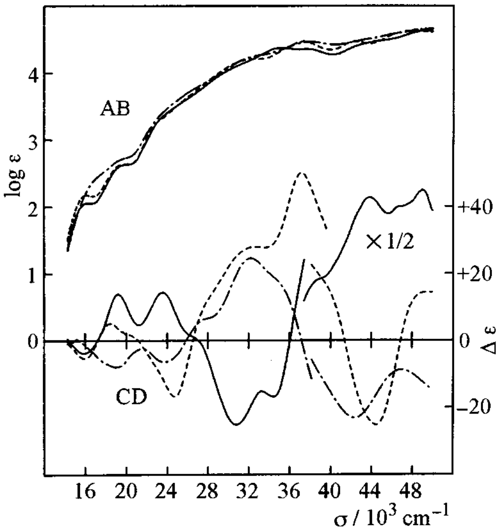

Figure 3. Absorption and CD spectra of [**4a**]$^{2+}$ (ΛΛ$_D$-[**4**]$^{2+}$) (—), [**4b**]$^{2+}$ (ΔΛ$_D$-[**4**]$^{2+}$) (— • —), and [**4c**]$^{2+}$ (ΔΔ$_D$-[**4′**]$^{2+}$) (- - -) in H$_2$O.

The absorption and CD spectra of [**4c**]$^{2+}$ are compared with those of ΛΛ$_D$- and ΔΛ$_D$-[**4**]$^{2+}$ in Figure 3; the extinction coefficient for [**4c**]$^{2+}$ was tentatively adjusted so as to have the same value for ΛΛ$_D$-[**4**]$^{2+}$ at 36.0×10^3 cm^{-1}. The absorption spectral behavior of [**4c**]$^{2+}$ is similar to that of ΛΛ$_D$- and ΔΛ$_D$-[**4**]$^{2+}$, while its CD spectral curve is almost enantiomeric to that of ΛΛ$_D$-[**4**]$^{2+}$ over the whole region. These spectral features suggest that [**4c**]$^{2+}$ is the S-bridged Co^{III}Pt^{II}Co^{III} trinuclear complex composed of two *trans*(*N*)•*cis*(*O*)•*cis*(*S*)-[Co(N)$_2$(O)$_2$(S)$_2$]-type units with the Δ configuration. Molecular model examinations reveal that it is not possible for the D-pen ligand to adopt the tridentate-*N*,*O*,*S* coordination mode when the two *N*,*S*-chelate rings form the Δ configurational skew pair; the two COO$^-$ groups are situated in positions away from the remaining coordination sites of Co^{III}, because of the restriction of the *S* configurational carbon atom in the D-pen ligand (Figure 4). Accordingly, it is likely that [**4c**]$^{2+}$ has the S-bridged Co^{III}Pt^{II}Co^{III} trinuclear structure in ΔΔ$_D$-[Pt{Co(aet)$_2$(en)}{Co(D-pen-*N*,*S*)$_2$(H$_2$O)$_2$}]$^{2+}$, taking account of the 2+ formal charge

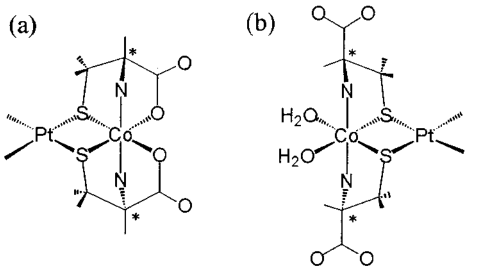

Figure 4. The model structure of the Λ configurational *trans*(*N*)-[Co(D-pen-*N*,*O*,*S*)$_2$]$^-$ unit (a) and that of the proposed Δ configurational *trans*(*N*)-[Co(D-pen-*N*,*S*)$_2$(H$_2$O)$_2$]$^-$ unit (b).

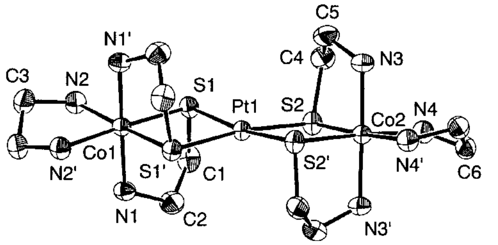

Figure 5. A perspective view of the complex cation [**1a**]$^{4+}$ (ΔΔ/ΛΛ-[**1**]$^{4+}$) with the atomic labeling scheme; the ΛΛ isomer is selected. Ellipsoids represent 50% probability.

Table 4. Selected Bond Distances (Å) and Angles (deg) for ΔΔ/ΛΛ-[**1**]Cl$_4$·6H$_2$O

	Distances		
Pt1−S1	2.312(2)	Co1−N2	2.001(6)
Pt1−S2	2.316(2)	Co2−S2	2.245(2)
Co1−S1	2.251(2)	Co2−N3	1.990(6)
Co1−N1	1.986(6)	Co2−N4	1.998(6)
	Angles		
S1−Pt1−S1′	84.03(9)	N2−Co1−N2′	85.5(4)
S1−Pt1−S2	96.53(6)	N4−Co2−N4′	85.4(4)
S1−Pt1−S2′	171.26(7)	S2−Co2−N4	176.7(2)
S2−Pt1−S2′	84.25(9)	S1−Co1−N2′	176.3(2)
S1−Co1−S1′	86.9(1)	N1−Co1−N1′	179.1(4)
S2−Co2−S2′	87.6(1)	Pt1−S1−Co1	94.54(7)
S1−Co1−N1	92.5(2)	Pt1−S2−Co2	94.09(7)
S2−Co2−N3	91.6(2)		

estimated from the column chromatographic behavior. That is, in [**4c**]$^{2+}$ the Pt^{II} center may be still bound by four S atoms from the two units; one is Δ-C_2-*cis*(*S*)-[Co(aet)$_2$(en)]$^+$, and the other is Δ$_D$-*trans*(*N*)-[Co(D-pen-*N*,*S*)$_2$(H$_2$O)$_2$]$^-$, having two aqua ligands in the place of carboxylate groups.

Crystal Structures of ΔΔ/ΛΛ-[Pt{Co(aet)$_2$(en)}$_2$]Cl$_4$·6H$_2$O ([1a]Cl$_4$·6H$_2$O) and ΔΛ-[Pt{Co(aet)$_2$(en)}$_2$]Cl$_4$·3H$_2$O ([1b]Cl$_4$·3H$_2$O). X-ray structural analysis for [**1a**]Cl$_4$·6H$_2$O revealed the presence of a discrete complex cation, four Cl$^-$ anions, and water molecules. The number of Cl$^-$ anions implies that the entire complex cation is tetravalent. The structure of the entire complex cation is shown in Figure 5, and its selected bond distances and angles are listed in Table 4. The complex cation [**1a**]$^{4+}$ consists of two *cis*(*S*)-[Co(aet)$_2$(en)]$^+$ units which are linked by a Pt atom through sulfur bridges to form a linear-type S-bridged trinuclear structure in [Pt{Co(aet)$_2$(en)}$_2$]$^{4+}$. The crystallographic 2-fold axis passing through Co1, Pt1, and Co2 atoms requires that the three metal atoms are arranged to be exactly linear. The geometry about each terminal Co atom is approximately octahedral, coordinated by two aet S and two en N atoms in the equatorial positions and two aet N atoms at apical positions to have a C_2 symmetry. Considering the chiral configurations (Δ and Λ) of each C_2-*cis*(*S*)-[Co(aet)$_2$(en)]$^+$ unit, three isomers (ΔΔ, ΛΛ, and ΔΛ) are possible for [Pt{Co(aet)$_2$(en)}$_2$]$^{4+}$. The crystal of [**1a**]Cl$_4$·6H$_2$O consists of the ΔΔ and ΛΛ isomers, which combine to form the racemic compound; the ΛΛ isomer is selected in Figure 5. This is in line with the fact that [**1a**]$^{4+}$ was optically resolved with use of [Sb$_2$(*R*,*R*-tartrato)$_2$]$^{2-}$ as the resolving agent. The central PtS$_4$ sphere is distorted from square-planar to tetrahedral geometry, in which the S1−Pt1−S1′ and S2−Pt1−S2′ planes intersect to form a dihedral angle of 13.1°. A similar distortion has been observed for ΔΔ/ΛΛ-[M{Co(aet)$_2$(en)}$_2$]$^{4+}$ (M = Ni^{II}, Pd^{II}),[27,28] and it has been pointed out that this distortion allows the methylene protons of the aet chelate rings not to be located at the apical positions of the central metal atom.

Crystal [**1a**]Cl$_4$·6H$_2$O (ΔΔ/ΛΛ-[**1**]Cl$_4$·6H$_2$O) is isomorphous with ΔΔ/ΛΛ-[Ni{Co(aet)$_2$(en)}$_2$]Cl$_4$·6H$_2$O and ΔΔ/ΛΛ-[Pd{Co(aet)$_2$(en)}$_2$]Cl$_4$·6H$_2$O, in which the central Ni^{II} or Pd^{II} atom is bound by two C_2-*cis*(*S*)-[Co(aet)$_2$(en)]$^+$ units.[27,28] Thus, the direct comparison of the structural parameters for M = Ni^{II}, Pd^{II}, and Pt^{II} coordinated by the bidentate-*S*,*S* complex ligand, C_2-*cis*(*S*)-[Co(aet)$_2$(en)]$^+$, can be made. The M−S bond distances in ΔΔ/ΛΛ-[**1**]$^{4+}$, ΔΔ/ΛΛ-[Pd{Co(aet)$_2$(en)}$_2$]$^{4+}$, and ΔΔ/ΛΛ-[Ni{Co(aet)$_2$(en)}$_2$]$^{4+}$ average 2.314(2) Å, 2.310(1) Å, and 2.204(1) Å, respectively. This is in parallel with the covalent radii for Pd^{II} and Pt^{II}, which are evaluated to be essentially equal and larger than that for Ni^{II}.[33] The dihedral angles between two MS$_2$ trigonal planes decrease in the order M = Ni^{II} (16.2°) > Pd^{II} (14.0°) > Pt^{II} (13.1°), indicative of the preference of square-planar geometry over tetrahedral geometry on going from Ni^{II} to Pd^{II} and from Pd^{II} to Pt^{II}. On the other hand, the bond distances and angles concerning the C_2-*cis*(*S*)-[Co(aet)$_2$(en)]$^+$ units for the three Co^{III}MCo^{III} complexes are quite similar to each other, although the Co−S bond distances for ΔΔ/ΛΛ-[Ni{Co(aet)$_2$(en)}$_2$]$^{4+}$ (average 2.238(1) Å) are somewhat shorter than those for ΔΔ/ΛΛ-[Pd{Co(aet)$_2$(en)}$_2$]$^{4+}$ (average 2.246(1) Å) and ΔΔ/ΛΛ-[**1**]$^{4+}$ (average 2.248(2) Å), presumably due to the weaker Ni−S bonds.

X-ray analysis established that the complex cation of [**1b**]Cl$_4$·3H$_2$O also has the S-bridged Co^{III}Pt^{II}Co^{III} trinuclear structure, in which the central Pt atom is coordinated by four S atoms from two octahedral C_2-*cis*(*S*)-[Co(aet)$_2$(en)]$^+$ units. The Pt−S bond distances (average 2.318(5) Å) in [**1b**]$^{4+}$ are essentially the same as those in [**1a**]$^{4+}$ (ΔΔ/ΛΛ-[**1**]$^{4+}$) (Table 5). As shown in Figure 6, a crystallographic center of symmetry is located at the Pt atom in [**1b**]$^{4+}$, and thus the two C_2-*cis*(*S*)-[Co(aet)$_2$(en)]$^+$ units have the Δ and Λ configurations to give the meso form. This is compatible with the fact that [**1b**]$^{4+}$ was not optically resolved by the same column chromatographic method used for [**1a**]$^{4+}$. The Pt atom is situated in a perfect square-planar environment, which differs markedly from the distorted square-planar geometry found in [**1a**]$^{4+}$. Furthermore, while the Pt atom

---

(33) Wells A. F. *Structural Inorganic Chemistry*, 5th ed.; Clarendon Press: Oxford, 1984.

Table 5. Selected Bond Distances (Å) and Angles (deg) for $\Delta\Lambda$-[**1**]$Cl_4 \cdot 3H_2O$

	Distances		
Pt1−S1	2.317(5)	Co1−N1	1.97(2)
Pt1−S2	2.318(4)	Co1−N2	1.98(2)
Co1−S1	2.234(5)	Co1−N3	1.96(2)
Co1−S2	2.253(5)	Co1−N4	1.99(2)
	Angles		
S1−Pt1−S2	82.6(2)	S1−Co1−N4	176.4(5)
S1−Pt1−S2′	97.4(2)	S2−Co1−N3	177.7(5)
S1−Co1−S2	86.0(2)	N1−Co1−N2	175.8(7)
S1−Co1−N1	88.3(5)	Pt1−S1−Co1	95.0(2)
S2−Co1−N2	86.5(5)	Pt1−S2−Co1	94.5(2)
N3−Co1−N4	85.3(7)		

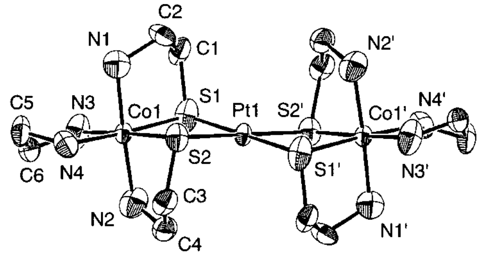

Figure 6. A perspective view of the complex cation [**1b**]$^{4+}$ ($\Delta\Lambda$-[**1**]$^{4+}$) with the atomic labeling scheme. Ellipsoids represent 50% probability.

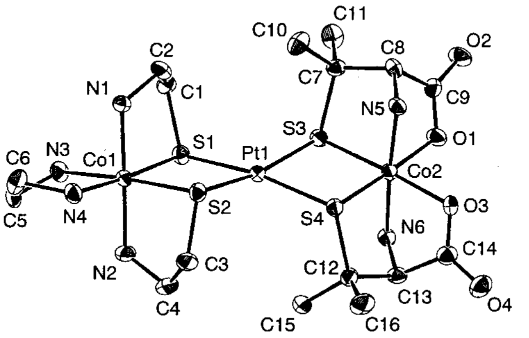

Figure 7. A perspective view of the complex cation [**4b**]$^{2+}$ ($\Delta\Lambda_{\mathrm{D}}$-[**4**]$^{2+}$) with the atomic labeling scheme. Ellipsoids represent 50% probability.

lies almost on the same plane made by each CoS_2 trigonal plane in [**1a**]$^{4+}$, two pairs of adjacent CoS_2 and PtS_4 planes are not coplanar in [**1b**]$^{4+}$, yielding a flat chairlike conformation for which the folding angle between each CoS_2 plane and the PtS_4 plane along the common S−S line is 166.0°. Molecular model examinations reveal that in the meso form there exists a cross-plane interaction between the aet chelate rings of the two C_2-*cis*(*S*)-[Co(aet)$_2$(en)]$^+$ units,[27b] which is effectively decreased by the bending of the two pairs of adjacent planes along the common S−S line.

Crystal Structure of $\Delta\Lambda_{\mathrm{D}}$-[Pt{Co(aet)$_2$(en)}{Co(D-pen-*N,O,S*)$_2$}]$Cl_2 \cdot 6H_2O$ ([4b]$Cl_2 \cdot 6H_2O$). X-ray structural analysis of [**4b**]$Cl_2 \cdot 6H_2O$ showed the presence of a discrete divalent complex cation, two chloride anions, and water molecules. The structure of the complex cation [**4b**]$^{2+}$ is shown in Figure 7, and its selected bond distances and angles are summarized in Table 6. The complex cation [**4b**]$^{2+}$ is composed of C_2-*cis*(*S*)-[Co(aet)$_2$(en)]$^+$ and a *trans*(*N*)-[Co(D-pen-*N,O,S*)$_2$]$^-$ octahedral units that are linked by the central Pt atom to give an S-bridged trinuclear structure in [Pt{Co(aet)$_2$(en)}{Co(D-pen-*N,O,S*)$_2$}]$^{2+}$. Complex [**4b**]$^{2+}$ has no crystallographically imposed symmetry, but an idealized C_2 axis passes though Co1, Pt1, and Co2 atoms. In [**4b**]$^{2+}$, the Pt1−S3 and Pt1−S4 bond distances average 2.349(3) Å, which is ca. 0.03 Å longer than the averaged distance of Pt1−S1 and Pt1−S2 (2.320(3) Å). On the other hand, the averaged bond distance of Co2−S3 and Co2−S4 (2.223(3) Å) is ca. 0.03 Å shorter than that of Co1−S1 and Co1−S2 (2.250(3) Å). This comparison suggests that the thiolato S atoms in the *trans*(*N*)-[Co(D-pen-*N,O,S*)$_2$]$^-$ unit have a coordination ability slightly lower than have the S atoms in the C_2-*cis*(*S*)-[Co(aet)$_2$(en)]$^+$ unit, owing to the greater donation toward the Co^{III} center. The absolute configuration for the C_2-*cis*(*S*)-[Co(aet)$_2$(en)]$^+$ unit in [**4b**]$^{2+}$ is Δ, which is determined on the basis of the known *S* configuration of the asymmetric carbon atom in the D-pen ligand, together with the Flack parameter (−0.0047(2)).[34] Thus, [**4b**]$^{2+}$ has a pseudo meso form of $\Delta\Lambda_{\mathrm{D}}$, considering the Λ configurational skew pair of the two five-membered *N,S*-chelate rings in the *trans*(*N*)-[Co(D-pen-*N,O,S*)$_2$]$^-$ unit (Figure 7). The bond distances and angles concerning the C_2-*cis*(*S*)-[Co(aet)$_2$(en)]$^+$ and Λ_{D}-*trans*(*N*)-[Co(D-pen-*N,O,S*)$_2$]$^-$ units in [**4b**]$^{2+}$ are quite similar to those found in the related $Co^{III}Pd^{II}Co^{III}$ trinuclear complex, $\Lambda\Lambda_{\mathrm{D}}$-[Pd{Co(aet)$_2$(en)}{Co(D-pen-*N,O,S*)$_2$}]$^{2+}$.[29] However, the geometry about the central Pt atom in [**4b**]$^{2+}$ is significantly distorted from square-planar to tetrahedral geometry, compared with that in $\Lambda\Lambda_{\mathrm{D}}$-[Pd{Co(aet)$_2$(en)}{Co(D-pen-*N,O,S*)$_2$}]$^{2+}$; the dihedral angles between the two MS_2 planes for [**4b**]$^{2+}$ and $\Lambda\Lambda_{\mathrm{D}}$-[Pd{Co(aet)$_2$(en)}{Co(D-pen-*N,O,S*)$_2$}]$^{2+}$ are 16.3° and 8.4°, respectively. Molecular model studies point out that this distortion minimizes the cross-plane interaction between the methyl groups of the D-pen ligands and the methylene groups of the aet ligands which exists in the $\Delta\Lambda_{\mathrm{D}}$-configurational S-bridged trinuclear structure.

Table 6. Selected Bond Distances (Å) and Angles (deg) for $\Delta\Lambda_{\mathrm{D}}$-[**4**]$Cl_2 \cdot 6H_2O$

	Distances		
Pt1−S1	2.322(3)	Co1−N3	1.987(8)
Pt1−S2	2.318(3)	Co1−N4	1.992(9)
Pt1−S3	2.353(3)	Co2−S3	2.237(3)
Pt1−S4	2.345(3)	Co2−S4	2.208(3)
Co1−S1	2.265(3)	Co2−O1	1.941(7)
Co1−S2	2.234(3)	Co2−O3	1.970(7)
Co1−N1	1.971(9)	Co2−N5	1.928(9)
Co1−N2	1.970(9)	Co2−N6	1.947(9)
	Angles		
S1−Pt1−S2	81.68(9)	S3−Co2−O1	90.1(3)
S1−Pt1−S3	98.37(9)	S3−Co2−O3	177.0(2)
S1−Pt1−S4	170.11(10)	S3−Co2−N5	88.5(3)
S2−Pt1−S3	168.48(9)	S4−Co2−O1	176.9(2)
S2−Pt1−S4	99.19(9)	S4−Co2−O3	90.5(2)
S3−Pt1−S4	82.76(9)	S4−Co2−N6	88.6(3)
S1−Co1−S2	84.8(1)	O1−Co2−N5	82.0(3)
S1−Co1−N1	87.7(3)	O1−Co2−N5	82.0(3)
S1−Co1−N4	175.6(3)	O3−Co2−N6	83.6(3)
S2−Co1−N1	92.4(3)	N5−Co2−N6	175.7(4)
S2−Co1−N2	87.5(3)	Pt1−S1−Co1	96.2(1)
S2−Co1−N3	175.3(3)	Pt1−S2−Co1	97.2(1)
N1−Co1−N2	178.1(4)	Pt1−S3−Co2	93.8(1)
N3−Co1−N4	85.3(4)	Pt1−S4−Co2	94.8(1)
S3−Co2−S4	88.6(1)		

---

[34] (a) Flack, H. D. *Acta Crystallogr., Sect. A* **1983**, *39*, 876. (b) Flack, H. D.; Bernandinello, G. *Acta Crystallogr., Sect. A* **1985**, *41*, 500.

Concluding Remarks

In the present study, the 1:1 reaction of the racemic ΔΔ/ΛΛ-[Ni{Co(aet)$_2$(en)}$_2$]$^{4+}$ with [PtCl$_4$]$^{2-}$ was found to produce both the racemic (ΔΔ/ΛΛ) and meso (ΔΛ) forms of [Pt{Co(aet)$_2$(en)}$_2$]$^{4+}$ ([**1**]$^{4+}$), which implies that the intermolecular rearrangement of the C_2-*cis*(*S*)-[Co(aet)$_2$(en)]$^+$ units occurs in the course of the metal replacement reaction. This result is in sharp contrast to the selective formation of the racemic form for [Pd{Co(aet)$_2$(en)}$_2$]$^{4+}$ by the corresponding reaction with [PdCl$_4$]$^{2-}$.[28] The MM2 calculations for the meso and racemic forms of [**1**]$^{4+}$,[35] which were carried out with use of the fixed atomic coordinates obtained by X-ray analyses, indicate that the meso form would be of significantly higher energy than the racemic form by ca. 55 kJ mol^{-1}. Thus, it is reasonable to assume that the thermodynamically unstable meso form created at the first stage converts to the racemic form for [Pd{Co(aet)$_2$(en)}$_2$]$^{4+}$ because of the kinetically lability of the Pd−S bonds, while the inertness of the Pt−S bonds prevents the meso form from converting to the racemic form for [Pt{Co(aet)$_2$(en)}$_2$]$^{4+}$. Indeed, the 1:1 reaction of Δ/Λ-[PtCl$_2${Co(aet)$_2$(en)}]$^+$ ([**2**]$^+$) with Λ$_{\rm D}$-*trans*(*N*)-[Co(D-pen-*N*,*O*,*S*)$_2$]$^-$ was found to produce the sterically unfavorable ΔΛ$_{\rm D}$ isomer of [Pt{Co(aet)$_2$(en)}{Co(D-pen-*N*,*O*,*S*)$_2$}]$^{2+}$ ([**4**]$^{2+}$), besides its ΛΛ$_{\rm D}$ isomer, while [Pt{Co(aet)$_2$(en)}$_2$]$^{4+}$ ([**1**]$^{4+}$) and Λ$_{\rm D}$Λ$_{\rm D}$-[Pd{Co(D-pen-*N*,*O*,*S*)$_2$}$_2$]^0 (Λ$_{\rm D}$Λ$_{\rm D}$-[**3**]) were formed only slightly. On the other hand, it has been shown that the corresponding reaction of Δ/Λ-[PdCl$_2${Co(aet)$_2$(en)}]$^+$ with Λ$_{\rm D}$-*trans*(*N*)-[Co(D-pen-*N*,*O*,*S*)$_2$]$^-$ results in the chiral selective formation of the ΛΛ$_{\rm D}$ isomer for [Pd{Co(aet)$_2$(en)}{Co(D-pen-*N*,*O*,*S*)$_2$}]$^{2+}$, together with ΔΔ-[Pt{Co(aet)$_2$(en)}$_2$]$^{4+}$ and Λ$_{\rm D}$Λ$_{\rm D}$-[Pd{Co(D-pen-*N*,*O*,*S*)$_2$}$_2$]^0 (Scheme 1).[29] Accordingly, it is concluded that not only the thermodynamic stability of isomers but also the kinetic lability of M−S bonds is the key to the chiral selective formation of the S-bridged Co^{III}MCo^{III} complexes composed of the bis(thiolato)-type octahedral Co^{III} units.

Supporting Information Available: X-ray crystallographic files, in CIF format, for the structure determination of ΔΔ/ΛΛ-[**1**]Cl$_4$·6H$_2$O, ΔΛ-[**1**]Cl$_4$·3H$_2$O, and ΔΛ$_{\rm D}$-[**4**]Cl$_2$·6H$_2$O. This material is available free of charge via the Internet at http://pubs.acs.org.

IC010696C

---

(35) (a) Allinger, N. L.; Yuh, Y. H. *QCPE* **1980**, *11*, 395. (b) Yoshikawa, Y. *J. Comput. Chem.* **1990**, *11*, 326.